Available online at www.eccomasproceedia.org
Eccomas Proceedia COMPDYN (2017) 1828-1842

ECCOMAS
Proceedia

COMPDYN 2017
6th ECCOMAS Thematic Conference on
Computational Methods in Structural Dynamics and Earthquake Engineering
M. Papadrakakis, M. Fragiadakis (eds.)
Rhodes Island, Greece, 15–17 June 2017

SEISMIC RESILIENCE ASSESSMENT OF THE WESTERN MACEDONIA HIGHWAY NETWORK IN GREECE

A. Sextos[1,2], I. Kilanitis[1], A. Kappos[1,3], M. Pitsiava[1], G. Sergiadis[1], V. Margaris[4], N. Theodoulidis[4], G. Mylonakis[2,5], P. Panetsos[6], K. Kyriakou[1]

[1]Aristotle University of Thessaloniki, Department of Civil Engineering, Greece
[2]University of Bristol, Department of Civil Engineering, United Kingdom
[3]City University London, Department of Civil Engineering, United Kingdom
[4] EPPO-ITSAK: Institute of Engineering Seismology & Earthquake Engineering, Greece
[5] University of Patras, Department of Civil Engineering, Greece
[6] Egnatia Odos S.A., Greece

Keywords: road networks, risk management, seismic retrofit, network resilience

ABSTRACT

Retis-Risk is a comprehensive framework recently developed for the assessment and management of the seismic resilience of interurban roadway networks. In this paper, this framework is applied for the road network of the prefecture of Western Macedonia in Greece. Refined data concerning real traffic conditions and network topology were collected and a detailed network mapping was performed in GIS. Utilizing an ad-hoc developed software for implementing the holistic methodology, the as-built road network was assessed and the network components with the highest vulnerability and consequence were identified. To improve the loss assessment reliability, bridge-specific fragility curves were employed based on the refined FE modeling. Structural and traffic cost due to earthquake scenarios of different return period were then predicted. To identify effective loss mitigation measures, the whole process was repeated assuming two different pre-earthquake risk management strategies. The first one concerns a retrofit program tailored to selected (i.e., the most critical) network components, while the second one focuses on the beneficial effect of a better recovery planning. Results indicate the significant contribution of an effective risk management to the loss mitigation and network resilience improvement. Moreover, a sustainable health monitoring system was installed on Polymylos bridge to ensure satellite data transmission during an earthquake event to update the post-earthquake recovery model, nearly in real time, with the measured spectral acceleration of the superstructure. The results indicate that the road network is adequately resilient, primarily due to its newly constructed infrastructure and its compliance to modern seismic standards. However, it consists an interesting application case demonstrating the applicability of the methodology and the major potential benefits of a holistic resilience-based management for the case similar intercity highway networks.

Peer-review under responsibility of the organizing committee of COMPDYN 2017.
doi: 10.7712/120117.5531.17692

1 INTRODUCTION

Recent strong earthquake events, including Chile 2010 and Tohoku 2011, among others, have shown that road network damage and traffic disruptions may substantially impair emergency response, rescue and recovery [1], [2]. At the same time, several cases have been reported wherein even minor damage to key network components had a disproportionally significant impact to the total amount of earthquake-induced loss. These facts have clearly shown that a significant part of the loss incurred by the community could have been averted should appropriate risk mitigation strategies had been adopted before the occurrence of the earthquake.

Since reducing exposure to seismic hazard by reallocating structures is practically impossible for roadway networks that span over a wide area, emphasis should be placed on minimizing the potential earthquake consequences on the economy and society. An efficient planning for mitigating seismic risk of road networks [3]–[5] should involve a broad, system-perspective consideration that takes into account functionality and services rather than conventionally analyzing the structural performance of individual network components, such as bridges, tunnels and slopes. Moreover, the recovery process should be incorporated into the risk assessment, since it greatly influences the total amount of losses incurred.

Retis-Risk (www.retis-risk.eu) is a holistic framework developed for the seismic risk assessment and resilience enhancement of interurban roadway networks [6]. Utilizing a software tailored to the developed methodology, this paper describes its application of the for the case of the interurban roadway network of the Western Macedonia prefecture, in Greece. To illustrate the importance of post-disaster planning, two risk management strategies are considered and comparatively assessed; the first based on the identification and retrofit of the key components with the highest impact to network resilience and a second one, solely focusing on the improvement of recovery planning.

The study is bases on the actual data concerning network topology and traffic conditions which were collected and processed. Network bridge fragilities were taken into account in a refined manner utilizing a novel bridge-specific fragility methodology [7]. Tunnel fragility was also considered in the analysis, in an approximate manner through the description of a general tunnel fragility class [8].

Results indicate that the “as-built” road network is adequately resilient, primarily due to its newly constructed infrastructure and its compliance to modern seismic standards. However, the analysis of the two risk management strategies reveals the importance of quantifying resilience and then assessing alternative means to enhance loss mitigation and operation recovery. This study also demonstrates the applicability of the methodology as a whole in spotting key network components with the highest contribution to resilience, a process that is key in identifying the retrofit schemes with the maximum positive impact. Finally, the applicability of the methodology is further demonstrated by installing of a, satellite-based, monitoring system to a major bridge to provide nearly real-time post-earthquake spectral and free-field accelerations that can update the intensity measure distribution estimates after an earthquake event [9]. A summary of the methodology, the description of the network, the alternative enhancement strategies, as well as sample resilience assessment results are presented in the following.

2 ROAD NETWORK DESCRIPTION

2.1 Network Topology

"Εγνατία Οδός", often translated as Via Egnatia with code A2, extends from the western port of Igoumenitsa to the eastern Greek–Turkish border running a total of 670 km (420 mi). Egnatia Highway crosses the prefecture West Macedonia consisting the backbone of its road network, which is also complemented by several secondary roads that serve to the regional transportation needs (Fig. 1). Both the main highway of the region under study and the secondary road system with speed limits lower than 90km/h are modelled with a total number of 263 bidirectional links and 283 traffic nodes for the purposes of this analysis.

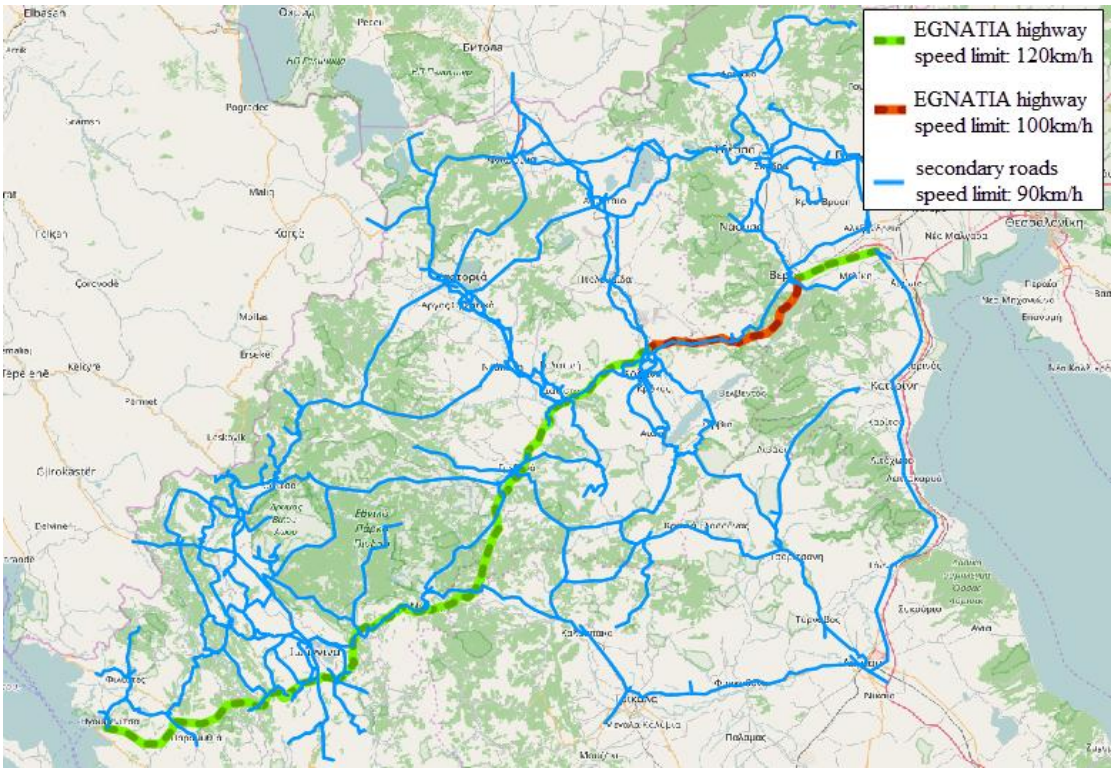

Figure 1: Case study road network

2.2 Key components of the network system

The set of *key network components*, that is, the structures whose failure may lead to road closures, is the first to be identified. Key components are assumed to be the bridges, overpasses, slopes and tunnels across the network. Given the structure of the interurban system studied, bridges and tunnels exist along the Egnatia highway only. Overpasses of the secondary network are also neglected for simplicity given their smaller size, simpler structural systems and minor effect to the overall network resilience. However, in principle, their vulnerability can be accounted for both by the methodology and the software developed, which are structure, size and importance-independent.

The key components locations were visually identified through Google Earth while their structural and geometrical characteristics were provided by Egnatia Highway

S.A. A total number of 148 key components were identified within the network system studied. Since the traffic along each network link is bi-directional, each identified key component comprises of two identical branches with a unique ID number per pair. Table 1 summarizes the ID, geographic latitude, longitude and length for the 46 bridge (and overpasses) and 28 tunnel pairs identified.

bridges & overpasses			
id	**φ**	**λ**	**length (m)**
b1	39.791	21.301	335
b2	39.793	21.303	133
b3	39.814	21.321	349
b4	39.836	21.329	203
b5	39.914	21.353	290
b6	39.926	21.363	200
b7	39.932	21.370	150
b8	39.965	21.373	158
b9	39.972	21.371	83
b10	39.981	21.369	636
b11	40.015	21.382	426
b12	40.033	21.405	326
b13	40.062	21.433	79
b14	40.081	21.447	97
b15	40.091	21.452	920
b16	40.110	21.461	76
b18	40.121	21.462	84
b19	40.166	21.502	200
b20	40.179	21.520	58
b21	40.196	21.520	280
b22	40.212	21.528	280
b23	40.225	21.552	27
b24	40.237	21.579	63
b25	40.307	21.695	57
b26	40.320	21.764	57
b27	40.346	21.797	100
b28	40.348	21.803	41
b30	40.349	21.806	81
b31	40.369	21.970	66
b32	40.368	22.047	30
b33	40.365	22.062	68
b34	40.365	22.068	60
b35	40.369	22.078	443
b36	40.378	22.093	247
b37	40.381	22.110	234
b38	40.388	22.146	170
b39	40.428	22.181	92
b40	40.455	22.210	166
b41	40.458	22.214	155
b42	40.504	22.228	46
b43	40.516	22.253	36
b44	40.542	22.319	132
b45	40.547	22.330	57
b46	40.586	22.470	37
b47	40.553	22.530	28
b48	40.556	22.593	91

tunnels			
id	**φ**	**λ**	**length (m)**
t0	39.805	21.308	2666
t1	39.816	21.323	1574
t2	39.844	21.334	335
t3	39.854	21.336	499
t4	39.865	21.338	719
t5	39.883	21.344	764
t6	39.910	21.354	642
t7	39.925	21.362	466
t8	39.931	21.368	423
t9	39.938	21.375	409
t10	39.947	21.380	1050
t11	39.958	21.380	768
t12	39.988	21.369	697
t13	40.175	21.511	286
t14	40.377	22.089	799
t15	40.381	22.100	491
t16	40.382	22.108	499
t17	40.384	22.127	2226
t18	40.392	22.156	180
t19	40.395	22.160	56
t20	40.403	22.168	337
t21	40.410	22.177	135
t22	40.426	22.182	241
t23	40.432	22.182	289
t24	40.439	22.181	237
t25	40.441	22.188	272
t26	40.457	22.214	274
t27	40.462	22.222	817

Table 1: Key network components

2.3 Pre-earthquake traffic conditions

An Origin-Destination (OD) matrix is used to describe the travel demands in the network for all possible combinations, extracted from a relevant study carried out by the stakeholder. Given the travel demands and the additional input of the traffic capacity of every network link, pre-earthquake traffic flows over the whole network are calculated according to [10]. It is noted that the OD matrix used herein, refers to travel demands during the typical hour of a normal day and thus appropriate scaling factors are applied to the results whenever daily traffic data are deemed.

2.4 Structural stock value, repair cost ratio, "traffic capacity-time" relationship

A re-construction cost was calculated for each one of the 74 dual branch key components assuming a value of 17.000€/m for the (twin) bridges and overpasses and 20.000€/m for the tunnels. Based on the length of each component, the total structural stock value of the network portfolio is approximately assessed to 630 million euros. Moreover, a damage state-specific repair cost ratio was defined for all the key components according to [11] assuming ratios of 0.03, 0.25, 0.75 and 1 for Damage State 1 (DS1) to Damage State 4 (DS4), respectively. A closure period of 0, 7, 150 and 450 days is further assigned to the four damage states, DS1 to DS4, for all key network components, assuming that after this period 100% of the traffic carrying capacity is regained.

3 SEISMIC HAZARD ANALYSIS

The integration of seismicity from different earthquake sources that is expressed in the form of conventional seismic hazard maps, is not applicable for the case of the post-earthquake traffic distribution, as the latter depends on the individual probability of operation of each network key component, which is in turn dependent on the specific seismic scenario examined and the corresponding spatial distribution of the Intensity Measures (IM) of interest [12], [13]. For this reason, hazard is herein assessed independently for each one of the m seismic sources potentially affecting the network and for a set of n different return periods.

Along these lines, eleven seismic sources (m=11) were identified, located either within the case study area or in its vicinity. These are named according to the seismic faults and the closest cities and towns as {"Kozani", "Kastoria", "Arta", "Ioannina", "Paramythia", "Anthemounta", "Larissa", "Edessa", "Koritsa", "Agrafa", "Stivos"}. For every fault, ground motion maps associated with the k=4 return periods, namely 100, 475, 980 and 1890 years, were generated leading to a sample of kxm maps depicting the spatial distribution of intensity.

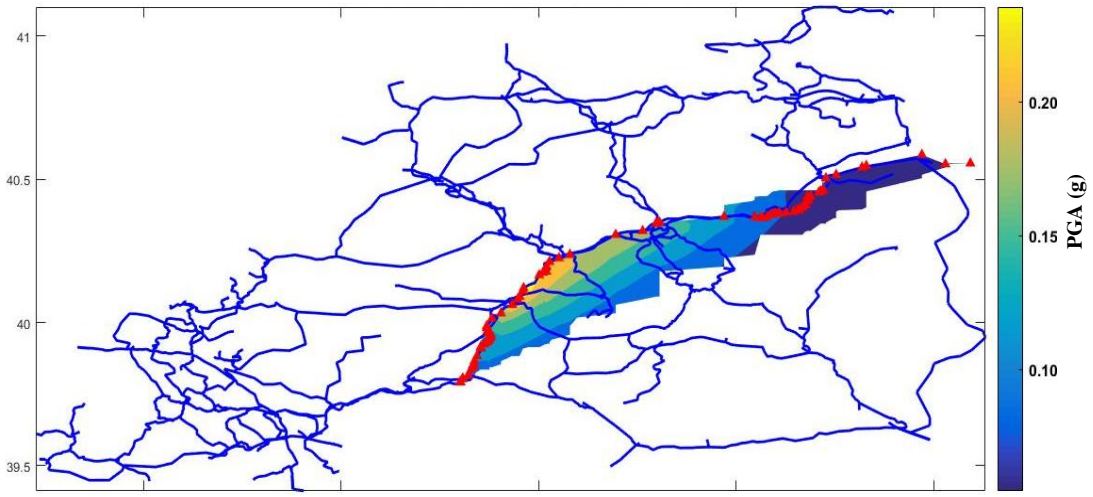

Figure 2: Sample seismic map associated with "Kozani" seismic source and a 475 year scenario.

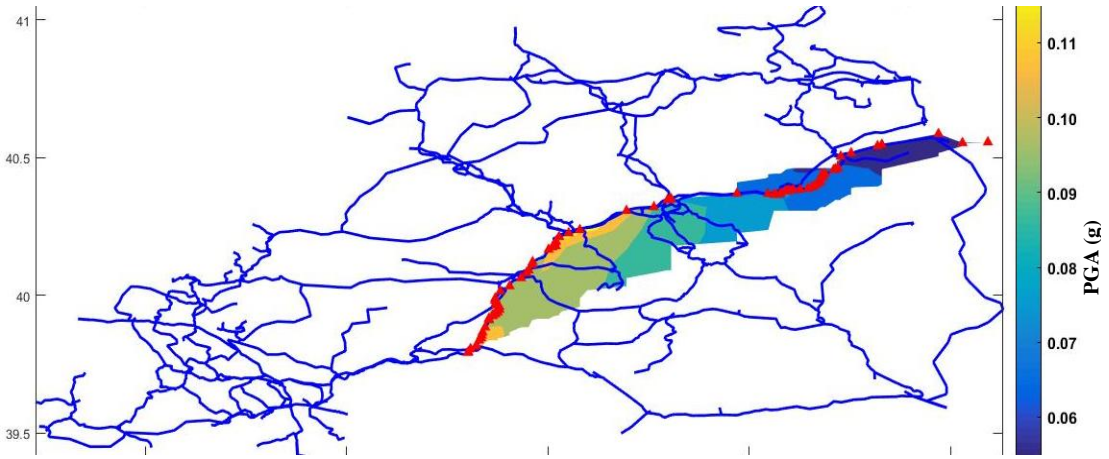

Figure 3: Sample seismic map associated with "Kastoria" seismic source and a 475 year scenario.

4 FRAGILITY ANALYSIS

For every bridge and overpass key component of this study, a set of four fragility curves was generated for the four damage states considered, DS1 to DS4, corresponding to minor, moderate, extensive damage and collapse, respectively (Fig. 4). Bridges and overpasses are organized in classes of identical fragility, while for important bridges of the network a bridge-specific methodology is followed [7] involving nonlinear static and incremental dynamic response history analysis. The stock of the 28 twin tunnels of the network was grouped into one gross tunnel fragility class also illustrated in Fig. 4 based on fragility relationships expressed in terms of peak ground velocity [8].

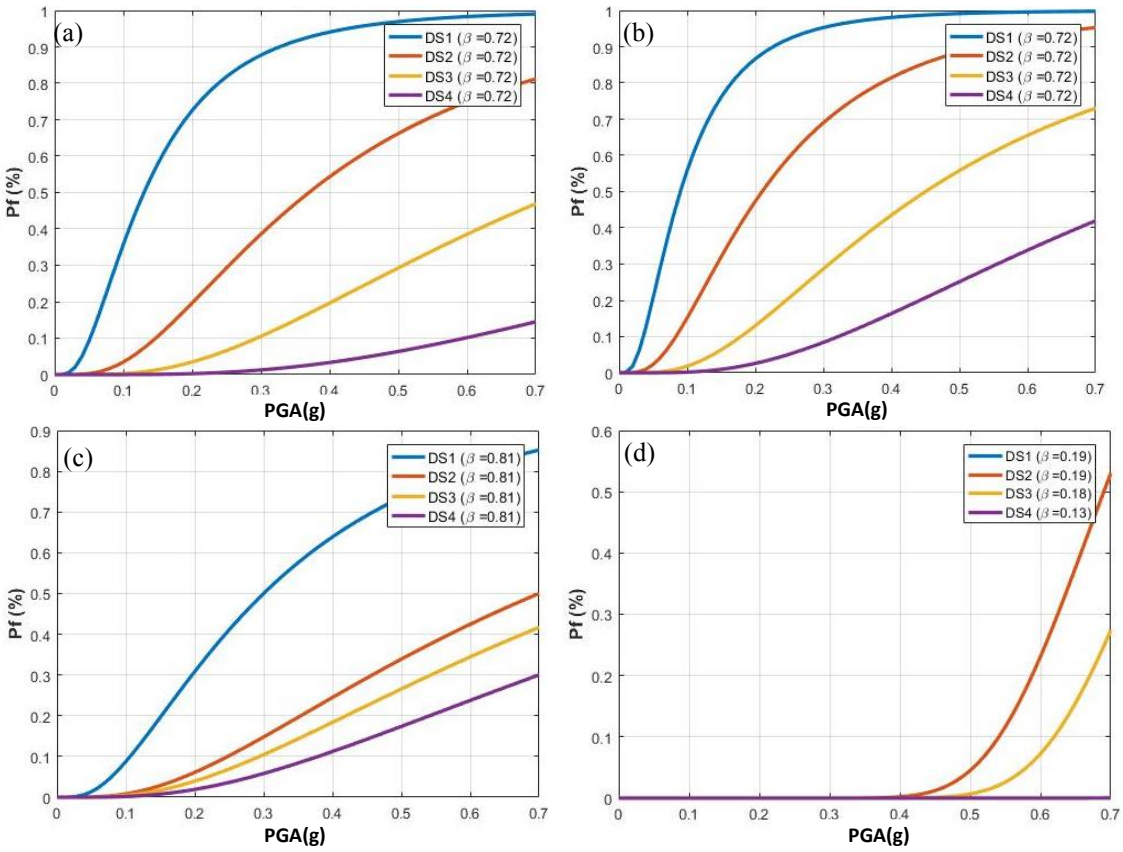

Figure 4: Bridge-specific fragility curves: bridges b1, b2 and b3 (charts a-c). General tunnel-class fragility curves (chart d)

In order to be consistent with the PGA-based maps developed, a transformation of PGV to PGA was performed according to [14]. Given the PGA value at the location of the key components, the probability that each component will experience damage corresponding to Damage States 1 to 4 was derived as follows:

$$P_{DS_0/PGA} = 1 - P_{S \geq DS_1/PGA}, P_{DS_1/PGA} = P_{S \geq DS_1/PGA} - P_{S \geq DS_2/PGA}$$
$$P_{DS_2/IM} = P_{S \geq DS_2/IM} - P_{S \geq DS_3/IM}, P_{DS_3/IM} = P_{S \geq DS_3/IM} - P_{S \geq DS_4/IM}, P_{DS_4/IM} = P_{S \geq DS_4/IM} \quad (1)$$

Figure 5 illustrates a sample fragility map showing the most probable Damage States of each key component on the basis of the probabilities computed by eq. (1) for the PGA values calculated for the seismic source “Kozani” and the return period of 475 years.

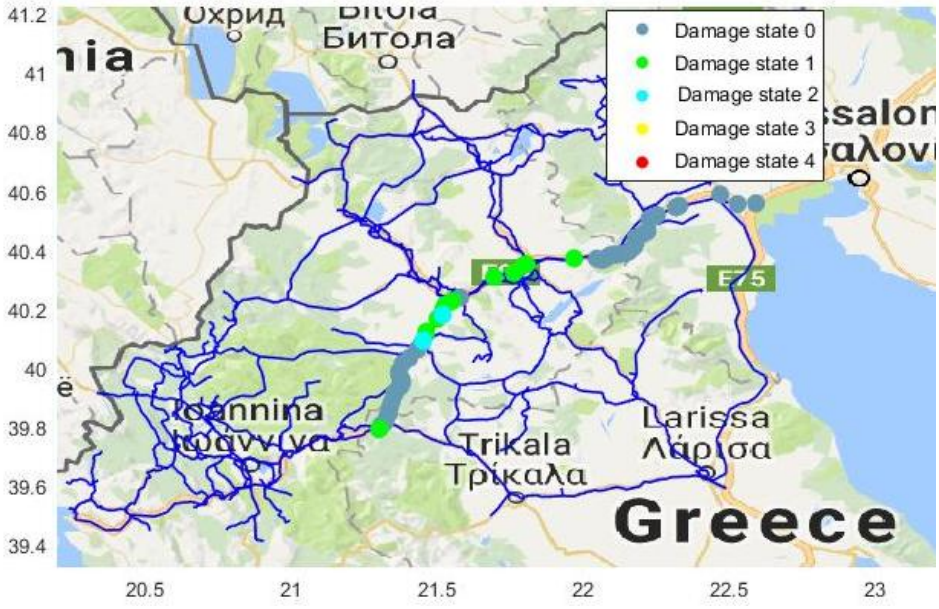

Figure 5: Sample fragility distribution map showing the most probable DS for every key component (seismic source: "Kozani", return period: 475 years)

5 TRAFFIC ANALYSIS

Having generated 11 different seismic maps for each return period, a corresponding set of traffic scenarios is then developed, under the assumption that immediately after an earthquake a key network component may either retain the 100% of its traffic carrying capacity (i.e., remain intact and hence, fully operational) or close and completely lose its traffic carrying capacity. Along these lines, each one of the 74 key components is assumed with a binary response, associated to a value of either 1 (fully functional) or 0 (closed) based on whether the damage induced exceeds a critical, moderate level of damage (DS_{cr}=DS_2). Given the individual Damage State probabilities computed by eq. (1), a Monte Carlo (MC) analysis is employed and 10 initial traffic scenario samples, each one consisting of a scheme defining open and closed network links, are associated to every PGA map. Hence, a group of 11x10=110 initial traffic scenarios is generated for each one of the four earthquake return periods.

Every initial traffic scenario is then decomposed to several phases that evolve in time based on the stepwise opening of the key components throughout the recovery period as shown in Figures 6 and 7. The latter decomposition of the initial (immediately after the earthquake) traffic scenario to *P=10* distinct post-earthquake phases is based on the "traffic carrying capacity vs. time" assumptions described in section 2.4.

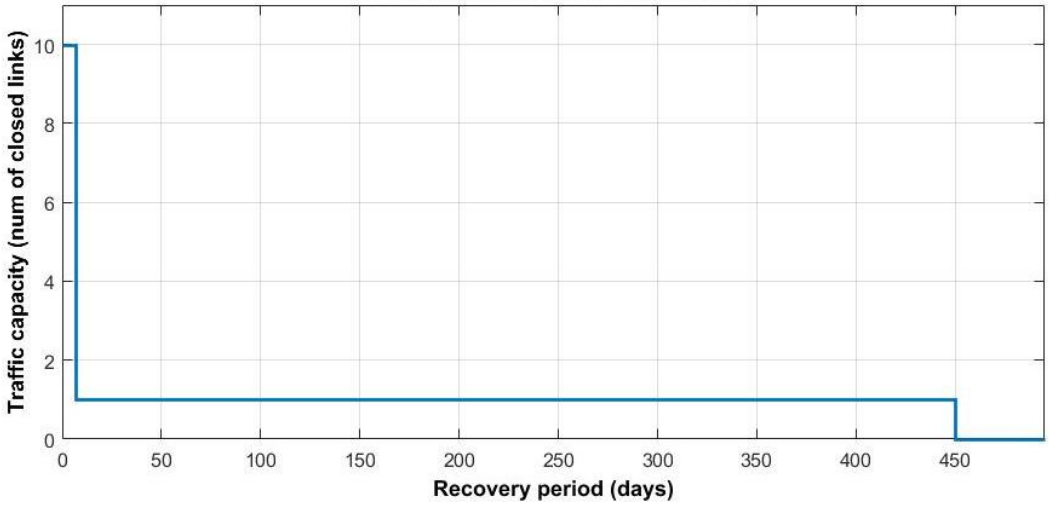

Figure 6: Number of closed links vs. time sampled from the 475 year map (seismic source: "Kozani").

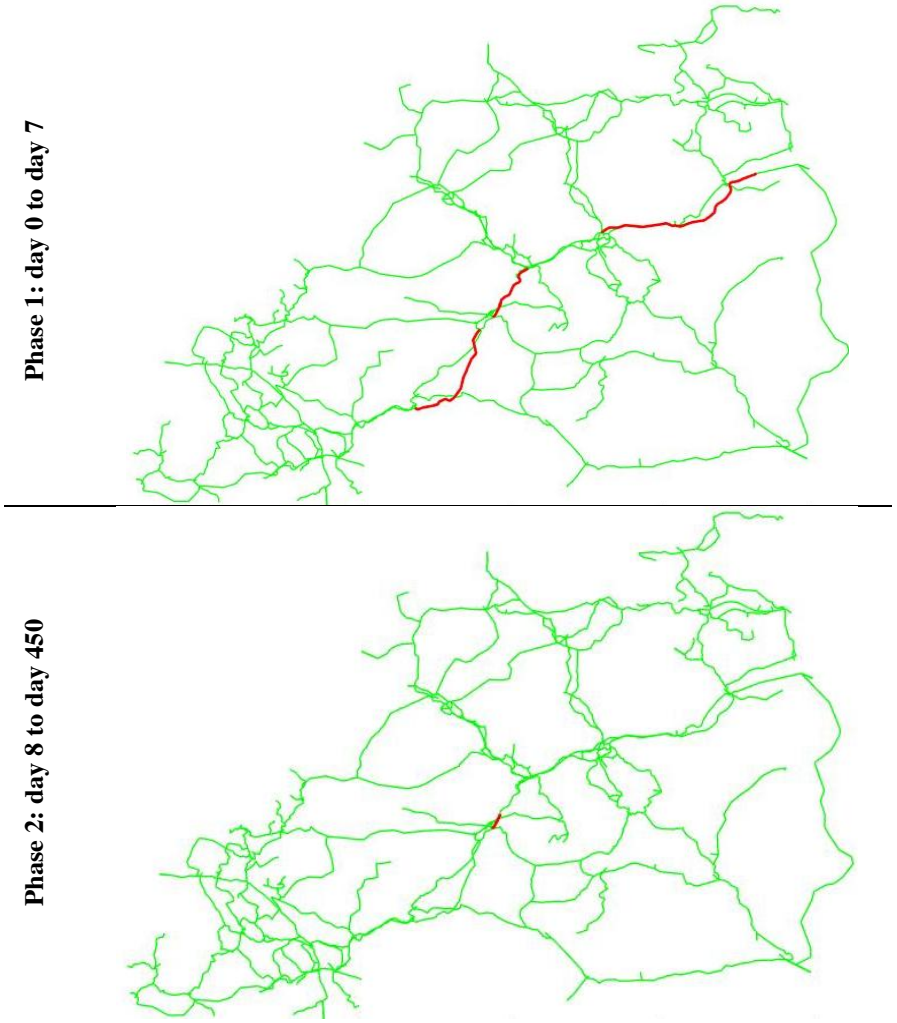

Figure 7: Distinct recovery phases within 7 days (top) and 8-450 days, corresponding to the initial traffic scenario sampled from the 475 year map of "Kozani" seismic source.

6 SEISMIC RISK ASSESMENT OF THE "AS-BUILT" NETWORK

The total cost associated with each earthquake event k (k taking values from 1 to 4 for the 100, 475, 980 and 1890 years return period), is the sum of the cumulative direct cost of structural damage within the network and the indirect, earthquake-induced total traffic cost. Based on the repair cost ratios defined in Section 2.4 and the probability of attaining every damage state, the Estimated Structural Cost $ESC_{k,m}$ due to earthquake k stemming from source m is derived for the i=74 key network components as:

$$ESC_{k,m} = \sum_{i=1}^{74} D_{i,k,m} \tag{2}$$

where:

$$D_{i,k,m} = TBC_i \cdot (RCR_1 \cdot P_{DS1}^{i,k,m} + RCR_2 \cdot P_{DS2}^{i,k,m} + RCR_3 \cdot P_{DS3}^{i,k,m} + RCR_4 \cdot P_{DS4}^{i,k,m}) \tag{3}$$

TBC_i: is the total cost of re-constructing key component i calculated based on its length (Table 1) and the re-construction cost per meter values defined in section 2.4,

$\{RCR_1^i, RCR_2^i, RCR_3^i, RCR_4^i\}$=$\{0.03,\ 0.25,\ 0.75,1\}$ are the repair cost ratios that correspond to damage states DS1 to DS4,

$P_{DS}^{i,k,m}$: is the probability that the damage of the key component i exceeds DS1 to DS4 for the case of n_{samp} seismic source m and an event return period k

The earthquake-induced traffic cost (TC) is calculated for every Monte Carlo simulated traffic scenario. This cost refers to the *additional* traffic cost during the entire recovery period of that particular traffic scenario (seismic source m and an event return period k), and as such, it is the sum of the product of each phase duration, times the corresponding additional travel cost:

$$TC_{k,m,n_{samp}} = \sum_{p=1}^{P_{k,m,n_{samp}}} EC_{k,m,n_{samp},p} \cdot t_{k,m,n_{samp},p} \tag{4}$$

where:

$EC_{k,m,n_{samp},p}$: is the *additional* travel cost due to travel delays during phase p of the n_{samp} traffic scenario sampled from the m^{th} IM distribution of earthquake k calculated according to [6]

$t_{k,m,n_{samp},p}$: is the duration of phase p of the n_{samp} traffic scenario sampled from the m^{th} IM distribution of event k

$P_{k,m,n_{samp}}$: is the total number of recovery phases associated with n_{samp} traffic scenario sampled from the m^{th} IM distribution of event k

Subsequently, the estimated traffic cost (ETC) can be associated to every seismic map, as the mean of the costs calculated for the 10 Monte Carlo samples (i.e., each one for each phase) simulated from that map:

$$ETC_{k,m} = \frac{\sum_{n_{samp}=1}^{10} TC_{k,m,n_{samp}}}{10} \tag{5}$$

The maximum of the estimated structural and traffic cost out of the 11 cases of individual seismic sources leads to the envelope total network cost (TNC_k) and identifies the *critical seismic source* that has the higher contribution to the overall loss among equiprobable possible costs corresponding to the 11 seismic sources:

$$TNC_k = \max_{m \in \overset{M}{1}} \left(ESC_{k,m} + ETC_{k,m} \right) \quad (6)$$

In the present case study, seismic source "Kozani" turn out to be the critical one among for all m=11 sources leading to a total network cost of TNC_k equal to 8.0, 24.6, 29.0, 33.6 million euros for return periods 100, 475, 980 and 1890 years respectively, (Fig. 8). It is worth mentioning that these values are very low (i.e., less than 5%) with respect to the total structural stock value of the network which was estimated to 630 million euros, thus implying that the network is considerably resilient to earthquakes. This is of course anticipated given the newly constructed and seismically designed Egnatial Highway key components. Moreover, traffic cost is low compared to the structural cost for all the return periods examined. This is because the probabilities of experiencing damage corresponding to DS3 and DS4 that lead to road closure and hence, to additional traffic cost are much lower than the probabilities of DS1 and DS2 (Fig. 5) that contribute only to the structural cost.

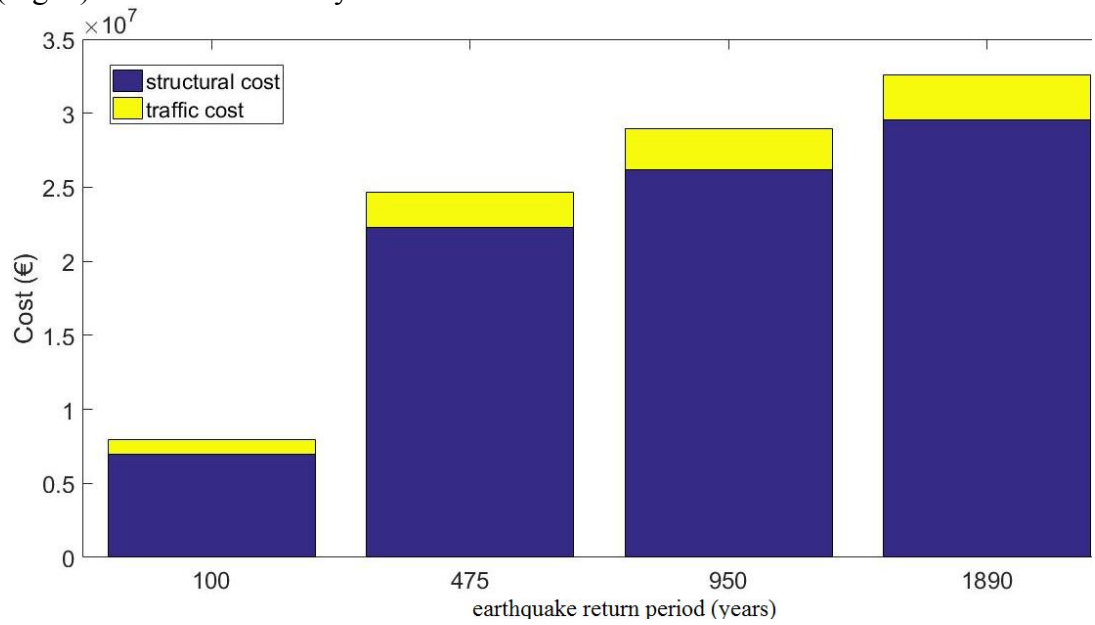

Figure 8: Expected structural and traffic cost for the four earthquake return period examined.

7 RISK MANAGEMENT STRATEGIES

For every Monte Carlo-sampled initial traffic scenario that is decomposed into phases, a plot showing network functionality evolution throughout the recovery period is generated. Every vertical branch of such a plot is associated to the opening of one or more links and respectively to one or more *critical key components* that are the last link components to open for the traffic (i.e. components that define the opening time of the whole link in case of a series of components comprising a link). Figure 9 shows the critical key components for the phases included in two indicative Monte Carlo samples.

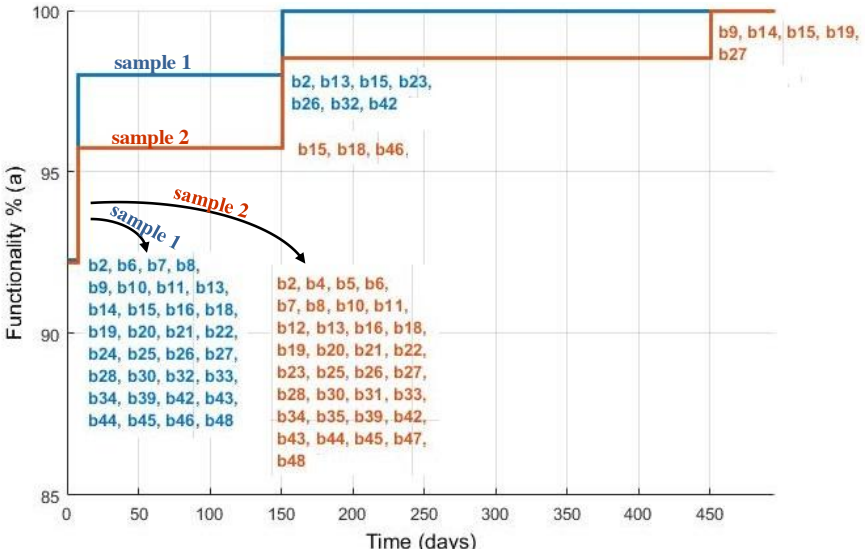

Figure 9: Identification of critical key components

The *highly-rated critical key components*, which are the components that are more frequently associated to vertical branches and influence at a greater extent the recovery of the network, have the higher impact to network resilience. Given the critical key components for all the phases throughout a properly defined pool of functionality plots, a retrofit scheme targeting the specific highly-rated critical key components for that pool can be defined. In this study, the pool of the 10 functionality plots associated to the 10 Monte Carlo samples sampled from the 1890 years return period event of the critical seismic source "Kozani, is used to define the retrofit plan. Key components b15, b18, b20, b21, b26 and b30 (Table 1) turn out to be critical 10 times throughout the $\sum_{nsamp=1}^{10} P_{4,1,n_{samp}} = 29$ phases included into the aforementioned pool of plots. A retrofit scheme therefore is developed for the particular bridges leading to updated fragilities or reduced probability of failure for the same Intensity Measure (Fig. 10). The updated fragilities were in this case approximately derived by multiplying the mean threshold value of the corresponding "as-built" components by 1.3, for all DSs.

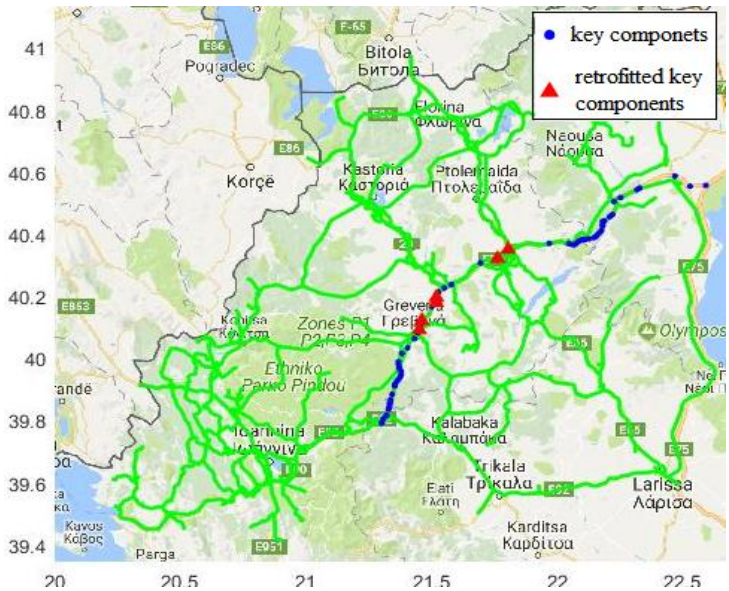

Figure 10: Targeted retrofit scheme involving seismic upgrade of six key components.

A second risk management strategy consisting of improved post-earthquake response expressed through an improved traffic carrying capacity-time relationship was also considered. In this case, closure periods were assumed to be lower due to better recovery planning and were updated to 0, 4, 100 and 300 days instead of 0, 7, 150 and 450 days for Damage States 1 to 4, respectively.

Figure 11 depicts the resulting estimated structural, traffic and total cost for different earthquake return periods for the case of the "as-built" network as well as the two risk management strategies (i.e., bridge retrofit or improved recovery planning) due to the seismic maps derived from the critical seismic source, as identified in Section 6.

Retrofit of selected key components is found to be more effective compared to the recovery plan enhancement for all the examined return periods. This is because, in this particular network, structural cost, which is essentially unaffected by an improved recovery, is the much higher than traffic cost. However, both risk management strategies contribute to a non-negligible, yet small (5-18%), extent to the the estimated total network cost reduction again due to the high resilience and low expected loss of the "as-built" network.

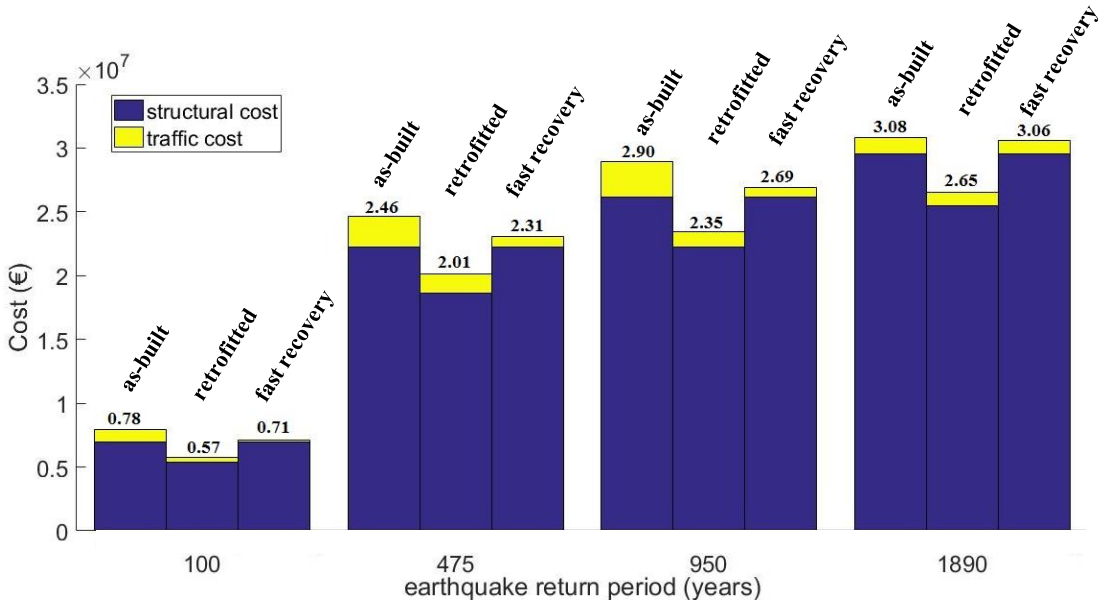

Figure 11: Expected costs for the four seismic scenarios for the case of the "as-built" network and the two risk mitigation stategies

8 STUCTURAL HEALTH MONITORING OF G9 BRIDGE

To further explore the possibility to update the intensity measure estimates with actual recordings after a major seismic event, a resilient structural health monitoring (SHM) scheme was installed to G9 bridge of the Egnatia motorway (b40 in Table 1) [9]. The system is based on serial/optical fiber data transfer from the data loggers to a local communication center, hybrid wired/cellular/satellite gateways from the local center to the end user, and uninterruptable power supply unit-based back up energy sources. The innovative elements this installation are the redundant end user gateways and the use of satellite communication that can provide crucial independence from terrestrial telecommunication networks. Nearly real-time data transmission can significantly improve the prediction of potentially damaged network components and

optimize the recovery actions of the first few hours. This pilot instrumentation is deemed a useful demonstration of the potential towards real-time estimation of seismic risk.

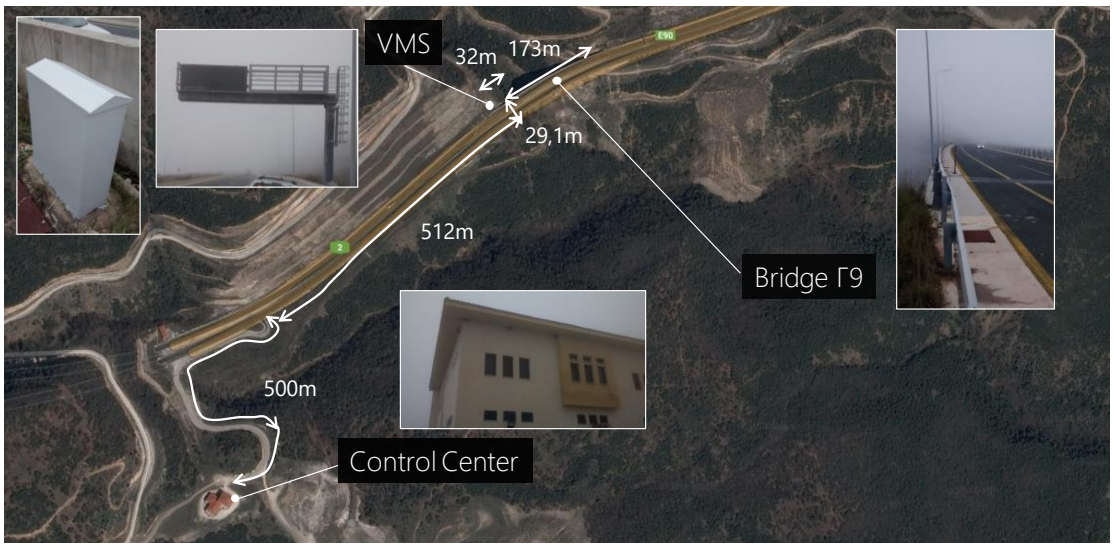

Figure 12: Layout of the monitoring scheme installed to G9 Egnaria Motorway bridge

9 CONCLUSIONS

In this paper an application is presented of the Retis-Risk framework (www.retis-risk.eu) for the case of the road network of Western Macedonia prefecture in Greece. After defining the network topology and pre-earthquake traffic conditions vulnerability of bridges and overpasses were taken into account in a refined way through the use of bridge-specific fragility curves. Tunnel fragility was also accounted for in the form of a general fragility class. The structural and traffic cost due to earthquakes of certain return periods was assessed for the existing network of the specific prefecture. The resilience of the network was found to be considerable mainly due to the recent construction of the high standard Egnatia Highway. For demonstration purposes, two alternative risk management strategies were also examined involving both a tailored retrofit scheme and an improved recovery planning strategy, the first being more effective by reducing loss by approximately up to 18%. This pilot study is deemed a useful example of the applicability of the Retis-Risk framework in assessing the seismic risk of interurban networks that can significantly enhance the informed decision-making of stakeholders, particularly of networks with a number of sub-standard key components and a more complex structure of interconnected roads.

REFERENCES

[1] K. Kawashima and I. Buckle, “Structural performance of bridges in the Tohoku-oki earthquake,” *Earthquake Spectra*, vol. 29, no. S1. pp. S315–S338, 2013.

[2] Y. Shen, B. Gao, X. Yang, and S. Tao, “Seismic damage mechanism and dynamic deformation characteristic analysis of mountain tunnel after Wenchuan earthquake,” *Eng*. *Geol*., vol. 180, pp. 85–98, 2014.

[3] C. Liu, Y. Fan, and F. Ordóñez, "A two-stage stochastic programming model for transportation network protection," *Comput. Oper. Res.*, vol. 36, no. 5, pp. 1582–1590, May 2009.
[4] S. Peeta, F. Sibel Salman, D. Gunnec, and K. Viswanath, "Pre-disaster investment decisions for strengthening a highway network," *Comput. Oper. Res.*, vol. 37, no. 10, pp. 1708–1719, Oct. 2010.
[5] P. Bocchini and D. M. Frangopol, "A probabilistic computational framework for bridge network optimal maintenance scheduling," *Reliab. Eng. Syst. Saf.*, vol. 96, no. 2, pp. 332–349, Feb. 2011.
[6] A. G. Sextos, I. Kilanitis, K. Kyriakou, and A. J. Kappos, "Resilience of Road Networks to Earthquakes," in *16th World Conference on Earthquake Engineering*, 2017.
[7] S. P. Stefanidou and A. J. Kappos, "Methodology for the development of bridge-specific fragility curves," *Earthq. Eng. Struct. Dyn.*, vol. 46, no. 1, pp. 73–93, 2017.
[8] A. Maravas and G. Mylonakis, "Fragility curves developed for the geotechnical components (Retis-Risk deliverable D3.1)," 2015.
[9] G. Sergiadis, S. Hadjidimitriou, V. Charisis, P. Panetsos, and T. Chrysanidis, "A structural health monitoring data managing scheme with resiliency to seismic events: Implementation on a road network bridge," in *COMPDYN 2015*.
[10] X. Zhou, J. Taylor, and F. Pratico, "DTALite: A queue-based mesoscopic traffic simulator for fast model evaluation and calibration," *Cogent Eng.*, vol. 1, no. 1, p. 961345, Dec. 2014.
[11] N. Basoz, A. S. Kiremidjian, S. A. King, and K. H. Law, "Statistical Analysis of Bridge Damage Data from the 1994 Northridge, CA, Earthquake," *Earthq. Spectra*, vol. 15, no. 1, pp. 25–54, 1999.
[12] J. Bommer and H. Crowley, "The Influence of Ground-Motion Variability in Earthquake Loss Modelling," *Bull. Earthq. Eng.*, vol. 4, no. 3, pp. 231–248, Mar. 2006.
[13] V. Sokolov, F. Wenzel, W.-Y. Jean, and K.-L. Wen, "Uncertainty and Spatial Correlation of Earthquake Ground Motion in Taiwan," *Terr. Atmos. Ocean. Sci.*, vol. 21, no. 6, pp. 905–921, 2010.
[14] D. J. Wald, V. Quitoriano, T. H. Heaton, and H. Kanamori, "Relationships between peak ground acceleration, peak ground velocity, and modified mercalli intensity in California," *Earthq. Spectra*, vol. 15, 3, pp. 557-564, 1999.